Fabrication of a Nanohybrid of Conjugated Polymer Nanoparticles and Graphene Oxide for Biosensing of Trypsin

Jaeguk Noh,[1] Byung-Jae Chae,[2] Bon-Cheol Ku,[3] Taek Seung Lee[1]

[1]Organic and Optoelectronic Materials Laboratory, Department of Advanced Organic Materials and Textile System Engineering, Chungnam National University, Daejeon 305-764, Korea
[2]Department of Chemistry, Chonbuk National University, Jeonju 561-756, Korea
[3]Institute of Advanced Composites Materials, Korea Institute of Science and Technology, Jeonbuk 565-905, Korea
Correspondence to: T. S. Lee (E-mail: tslee@cnu.ac.kr)

Received 20 February 2014; accepted 9 April 2014; published online 29 April 2014
DOI: 10.1002/pola.27215

ABSTRACT: Conjugated polymers containing triphenylamine group are synthesized via Suzuki coupling polymerization. Fluorescent-conjugated polymer nanoparticles (CPN) are prepared by reprecipitation method using the newly synthesized conjugated polymer. CPN can be encapsulated with polyarginine by electrostatic interaction. The CPN modified with polyarginine exhibit excellent interaction with graphene oxide (GO) which is chemically modified with hydrophilic groups that possesses negative charge, which, in turn, induces the quenching of the fluorescence of CPN upon formation of CPN–GO nanohybrid. Upon exposure to trypsin, the quenched fluorescence is recovered by release of CPN from the nanohybrid, because trypsin cleaves the polyarginine linkage, resulting in weakening of interaction between CPN and GO. © 2014 Wiley Periodicals, Inc. J. Polym. Sci., Part A: Polym. Chem. **2014**, *52*, 1898–1904

KEYWORDS: sensors; fluorescence; conjugated polymer nanoparticles; conjugated polymers; trypsin; graphene oxide

INTRODUCTION Recently, considerable demands on nanostructured materials such as fibers, particles, rods, tubes, and disks have been emerged for a variety of applications, including optoelectronics, multimodal imaging, and nanomedicine.[1] In particular, nanoparticles fabricated from conjugated polymers with unique properties,[2] such as high fluorescence, excellent photostability, good biocompatibility, and low cytotoxicity have provided new fluorescent probes for sensing and cellular imaging with proper surface modifications. The surface modification of CPN is known to be important in biology-related studies because the colloidal stability of CPN in aqueous solution is a primary concern.[3]

GO is a two-dimensional carbonaceous nanomaterial that can be readily prepared by an exfoliation process that forms monolayer sheets. Usually, GO has oxygen-based functional groups, including carboxylic acids, alcohols, and epoxides, leading to uniform dispersions in aqueous-based media, which have many applications.[4] Because GO nanosheets in aqueous dispersion possess negative charges on a hydrophobic backbone, positively charged molecules can be promptly adsorbed on the GO surface through electrostatic and $\pi-\pi$ interactions. Using this surface property of GO, many attempts to detect biologically related species have been carried out via turn-on or turn-off modes.[5] In these systems, charged species, such as polypeptides, proteins, and DNAs can facilely adsorb on to the GO surface via noncovalent interactions, which can be cleaved by external target species with more favorable interaction with GO.

As one of the proteases, trypsin is known to be an important digestive enzyme, and is produced in the pancreas as the proenzyme trypsinogen. The concentration of trypsin in the human body increases with some pancreatic diseases.[6] Thus, it is known that trypsin is overexpressed in pathological conditions of cancer and inflammation.[7] Moreover, as a kind of protease, trypsin can selectively cleave the carboxyl chain of amino acids such as lysine or arginine.[8]

In this work, we demonstrate a new, versatile CPN material for the analysis of a specific protein, trypsin, while GO is used as an effective quencher. The fluorescence quenching by GO follows a surface energy transfer process, rather than a Förster resonance energy transfer (FRET) mechanism, which does not require the spectral overlap between the energy donor and the acceptor, enabling wide selection window of the energy donor.[9] Fabrication of a nanohybrid, comprised CPN and GO, was successfully carried out through electrostatic assembly, via preparation of surface-modified CPN with polyarginine (pArg), which made the CPN positively charged and thus acted as a linker for both CPN and

Additional Supporting Information may be found in the online version of this article.

GO. By constructing a hybrid of GO and pArg-encapsulated CPN, quenching could be observed because of the presence of the energy-accepting GO. Because trypsin selectively degrades the linker pArg, recovery of the initial fluorescence of CPN can be expected, thereby a selective trypsin detection method can be envisaged. The fluorescence-quenching property of GO depends on the ability of fluorescent species to immobilize on the GO surface, thus opening the possibility of constructing "turn-on" assay.[5,10(a–c)] To our knowledge, studies on the pArg-encapsulated CPN have seldom been reported.[10(d,e)] Besides, it is rare to introduce CPN into a quenching- and recovery-based fluorescence-sensing system with the aid of GO for the detection of protease.

EXPERIMENTAL

Materials

9,9-Dioctyl-2,7-dibromofluorene, 9,9-dioctylfluorene-2,7-diboronic acid bis(1,3-propanediol)ester, and tetrakis(triphenyl phosphine)-palladium(0) were purchased from Sigma-Aldrich and used without further purification. Polyarginine (mol. wt. 15,000–70,000) and trypsin (mol. wt. 23,300) were purchased from Sigma-Aldrich and used as received. 4-(*Bis*(4-bromophenyl)amino) benzaldehyde (**3**) was synthesized using previously published methods.[11] GO was prepared from graphite powder based on Hummer's method.[12]

Characterization

The ^{1}H NMR and ^{13}C NMR spectra were obtained on a Bruker DRX-300 spectrometer (Korea Basic Science Institute). Elemental analysis was performed with a CE Instruments EA-1110 elemental analyzer. The FT-IR spectra were recorded on a Bruker Tensor 27 spectrometer. The scanning electron microscope (SEM) images were obtained from Hitachi S-4800. The transmission electron microscope (TEM) images were obtained from JEOL JEM-3010. The image of atomic force microscope (AFM) was recorded on VEECO Nanoman. The UV–vis absorption spectra were recorded on a Perkin Elmer Lambda 35 spectrometer. The photoluminescence spectra were taken using a Varian Cary Eclipse spectrophotometer equipped with a xenon lamp excitation source.

Synthesis of Polymers

CP1: 3

(0.13 g, 0.30 mmol), 9,9-dioctyl-2,7-dibromofluorene (0.38 g, 0.70 mmol), 9,9-dioctylfluorene-2,7-diboronic acid *bis*(1,3-propanediol)ester (0.67 g, 1.20 mmol) were dissolved in a mixture of THF (10 mL) and 2 M aqueous potassium carbonate solution (4 mL). After addition of *tetrakis*(triphenylphosphine) palladium(0) (3.50 mg, 0.003 mmol), the reaction mixture was stirred under argon at 100 °C for 48 h. After the reaction, the reaction mixture was cooled and poured into methanol (500 mL), and resulting precipitates were isolated by filtration. The precipitates were washed with methanol and extracted with acetone for 48 h in a Soxhlet apparatus to remove oligomers and catalyst residues. The final product was yellowish powder (yield 0.35 g, 47%). ^{1}H NMR (300 MHz, $CDCl_3$) $\delta = 9.9$ (s), 7.8–6.9 (m), 4.1–3.7 (m), 2.8–2.0 (m), 1.6–1.0 (m) ppm. ^{13}C NMR ($CDCl_3$): $\delta = 191.2$, 146.6, 137.6, 133.1, 129.4, 112.7, 51.2, 31.1, 29.2, 27.9, 22.6. FT-IR (cm^{-1}): 3030 (C—H), 1697 (CH═O), 1591 (C═C), 1462(C═C), 1284 (C—N). Anal. calcd for $C_{50.92}H_{72.25}N_{0.27}O_{0.27}$: C 88.0, H 10.0, N 0.52; found: C 87.5, H 9.92, N 0.50.

CP2: 3

(0.215 g, 0.50 mmol), 9,9-dioctyl-2,7-dibromofluorene(0.274 g, 0.50 mmol), and 9,9-dioctylfluorene-2,7-diboronic acid *bis*(1,3-propanediol)ester (0.67 g, 1.20 mmol) were dissolved in a mixture of THF (10 mL) and 2 M aqueous potassium carbonate solution (4 mL). After addition of *tetrakis*(triphenylphosphine) palladium(0) (3.50 mg, 0.003 mmol), the reaction mixture was stirred under argon at 100 °C for 48 h. The reaction and work-up procedures are the same as the case for CP1. The final product was yellowish powder (yield 0.42 g, 51%). ^{1}H NMR (300 MHz, $CDCl_3$) $\delta = 9.8$ (s), 7.7–6.8 (m), 4.2–3.7 (m), 3.7–3.2 (m), 2.6–3.0 (m), 2.5–1.8 (m), 1.6–1.0 (m) ppm. ^{13}C NMR ($CDCl_3$): $\delta = 191.2$, 146.7, 137.6, 133.1, 129.3, 128.4, 112.8, 51.2, 27.9 ppm. FT-IR (cm^{-1}): 3028 (C—H), 1698 (CH═O), 1592 (C═C), 1461 (C═C), 1275 (C—N). Anal. calcd for $C_{50.4}H_{69.0}N_{0.4}O_{0.4}$: C 88.2, H 10.1, N 0.85; found: C 87.9, H 9.92, N 0.81.

CP3: 3

(0.30 g, 0.70 mmol), 9,9-dioctyl-2,7-dibromofluorene(0.17 g, 0.30 mmol), and 9,9-dioctylfluorene-2,7-diboronic acid *bis*(1,3-propanediol)ester (0.67 g, 1.20 mmol) were dissolved in a mixture of THF (10 mL) and 2 M aqueous potassium carbonate solution (4 mL). After addition of *tetrakis*(triphenylphosphine) palladium(0) (3.50 mg, 0.003 mmol), the reaction mixture was stirred under argon at 100 °C for 48 h. The reaction and work-up procedures are the same as the case for CP1. The final product was yellowish powder (yield 0.31 g, 43%). ^{1}H NMR (300 MHz, $CDCl_3$) $\delta = 9.9$ (s), 8.0–6.8 (m), 4.1–3.5 (m), 2.8–2.0 (m), 1.7–0.8 (m) ppm. ^{13}C NMR ($CDCl_3$): $\delta = 191.1$, 146.6, 137.3, 133.5, 129.7, 112.9, 51.1, 29.3, 27.9, 22.6. FT-IR (cm^{-1}): 3028 (C—H), 1697 (CH═O), 1593 (C═C), 1462 (C═C), 1323 (C—N). Anal. calcd for $C_{52.41}H_{66.25}N_{0.51}O_{0.51}$: C 89.0, H 9.31, N 1.10; found: C 88.59, H 9.23, N 1.01.

Preparation of CPN

Green-emitting CPN were prepared by reprecipitation method.[13] All experiments were performed in aqueous medium at room temperature. Typically, CP2 was first dissolved in THF to obtain 1 mg/mL stock solution. The CP2 solution (1 mL) was quickly added to Milli-Q water (12 mL) under vigorous sonication. Then, THF was removed by nitrogen stripping. The solution was filtered with 0.45-μm syringe filter. The aqueous medium containing dispersed CPN was transparent and stable for 2 weeks without any aggregation.

Preparation of pArg-Encapsulated CPN (pArg@CPN)

pArg was dissolved in water to prepare a stock solution (1 mg/mL). Then, 1 mL quantity of the pArg solution was

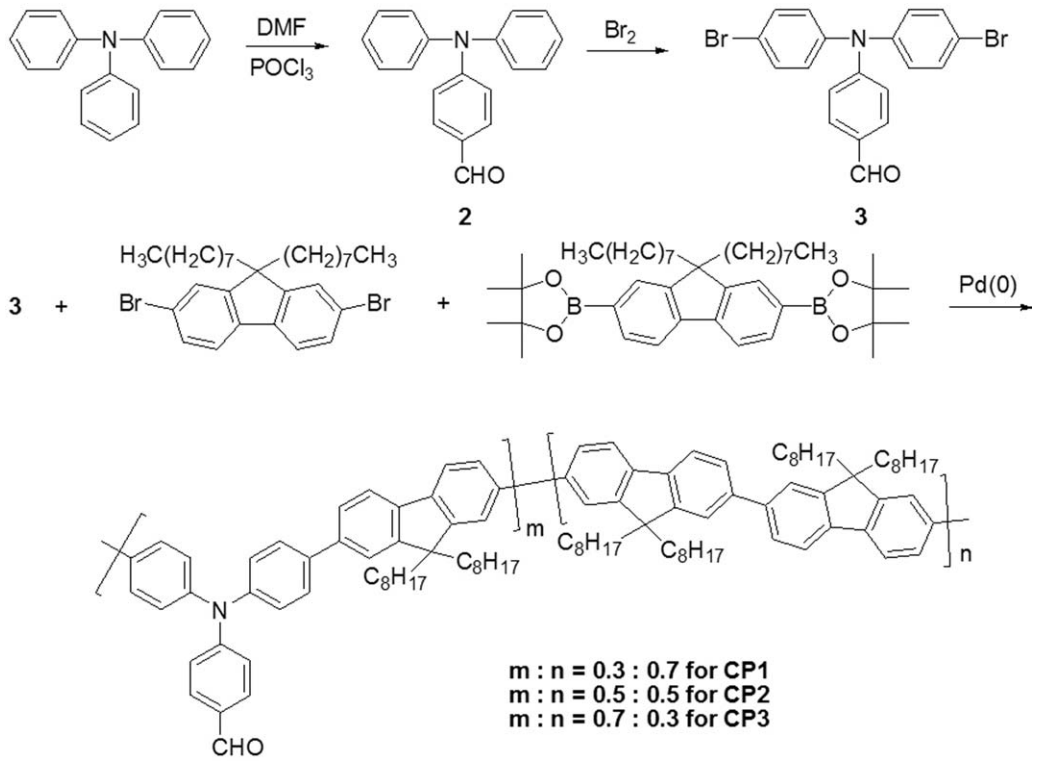

SCHEME 1 Synthetic routes for monomers and polymers.

added to aqueous CPN solution (10 mL) under a vigorous sonication. The mixture was further sonicated for 2 h. The aqueous solution of pArg@CPN was stored in a refrigerator to be used for the next step.

Trypsin Sensing

The sensing studies were carried out in a quartz cuvette with a path length of 10 mm. GO (20 μL) aqueous solution (100.1 μg/mL) was added to a dispersion of pArg@CPN (2.5 mL) in 20 mM HEPES buffer (pH = 7.4) and then the mixture was incubated for 5 min at room temperature. Then, trypsin was added into the solution. Subsequently, the solution was incubated at 37 °C for 40 min. Photoluminescence spectra of GO-pArg@CPN in the presence of the trypsin with various concentration were investigated.

RESULTS AND DISCUSSION

Scheme 1 shows the synthesis of the polymers, which are composed of a triphenylamine unit with a pendant aldehyde group and a fluorene moiety with long alkyl chains, exhibiting a reaction of **3**, 9,9-dioctylfluorene-2,7-diboronic acid bis(1,3-propanediol)ester, and 9,9-dioctyl-2,7-dibromofluorene via Suzuki coupling polymerization in the presence of a palladium catalyst. The structure of the polymer was confirmed by NMR and elemental analysis. The molar composition of each polymer was determined by elemental analysis and is tabulated in Table 1. All the polymers were soluble in common organic solvents such as THF, chloroform, and DMF. The molecular weights of the polymers were determined by gel permeation chromatography.

The absorption and emission spectra of the conjugated polymers in THF solutions are exhibited in Figure 1. The main absorption bands at 382 nm for CP1, 381 nm for CP2, and 383 nm for CP3 are attributed to the absorption of $\pi-\pi^*$ transitions of the polymer backbones, which are independent of the chemical composition of the backbone. In the fluorescence spectra, a major emission band at 490–501 nm assigned to aldehyde-containing triphenylamine units was observed for all the conjugated polymers. The intensity around 420 nm, assigned to the polyfluorene moiety, increases with the increase in the fluorene content in the polymers; its effect is dominant in CP1. In CP2 and CP3, stronger bluish green emissions from the aldehyde-containing triphenylamine groups are observed because of the energy transfer from fluorene units to aldehyde-containing triphenylamine groups.[14] Thus, the presence of electron-withdrawing aldehyde group is essential for exhibiting various emission colors by simple variation in feed ratios

TABLE 1 Properties of Conjugated Polymers

	Feed ratio (m:n)	Composition[a]	M_n[b]	M_w[b]	Polydispersity
CP1	0.3:0.7	0.27:0.73	6300	20,320	3.22
CP2	0.5:0.5	0.40:0.60	10,570	49,470	4.68
CP3	0.7:0.3	0.52:0.48	6680	19,220	2.88

[a] Determined by elemental analysis.
[b] Determined by GPC.

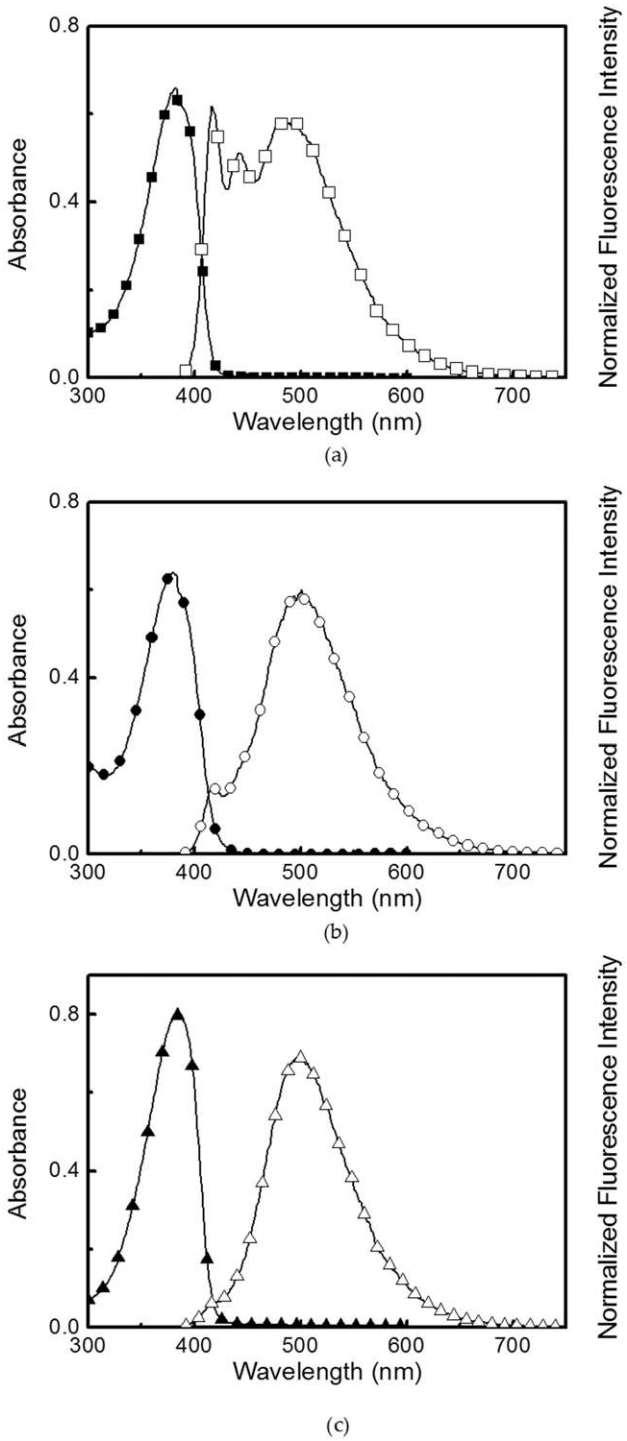

FIGURE 1 UV absorption (filled) and normalized fluorescence spectra (empty) of (a) CP1, (b) CP2, and (c) CP3 in THF solution (1×10^{-5} M for absorption of solutions). Excitation wavelength $\lambda_{ex} = 380$ nm.

of monomers. Furthermore, different from other electron-withdrawing groups, including carboxylic acid and sulfonic acid, aldehyde groups do not have electrolyte property, resulting in prevention of unfavorable, nonspecific interaction with biomolecules.

Subsequently, CPN of CP2 was prepared, using the conventional reprecipitation method, via the rapid addition of THF solution of CP2 to water. The spherical nanoparticles were successfully fabricated by the self-assembly of the hydrophobic polymer in the aqueous solution as shown in Figure 2(a). The particle size distribution of the CPN of CP2, determined by dynamic light scattering (DLS), is illustrated in Supporting Information Figure S1(a) and Supporting Information Table S1. A unimodal distribution can be observed for the solution of the CPN with a mean diameter of 37.02 nm. The photophysical properties of CP2 in THF solution and the CPN of CP2 in aqueous solution are compared in Supporting Information Figure S2. Both CP2 in THF solution and CPN in water showed very similar UV absorption (380 nm) and featureless, broad emission spectra centered at 491 nm, which emitted a bluish green light because of the broad emission in the long wavelength region. The quantum yields of CP2 in THF and CPN in water were measured as 43 and 23%, respectively, relative to rhodamine B in water.

The surface morphology of CPN in the presence of pArg was further investigated with TEM [Fig. 2(b)]. The CPN were successfully encapsulated by pArg (denoted as pArg@CPN); in this material, the pArg surrounds each CPN. It can be deduced that the negatively charged CPN were enveloped by positively charged pArg through electrostatic interaction. As expected, the average diameters of CPN determined by DLS changed from 37.02 to 53.26 nm after modification with pArg (Supporting Information Fig. S1 and Supporting Information Table S1). For better insight into the interaction between CPN and pArg, the zeta potentials for CPN before and after treatment of pArg were investigated. As depicted in Supporting Information Table S1, the net negative charge of the CPN (-34.6 mV) changed to $+47.8$ mV upon encapsulation with pArg. The strongly negatively and positively charged surfaces of the CPN and the resulting pArg@CPN, respectively, imply good stability in solution over a long period without precipitation.[15] The positive charges on the surface of pArg@CPN enabled further electrostatic interaction with negative GO.

GO was prepared using the modified Hummers method.[12] The prepared material nearly had a single layer with a topographic height of less than 2 nm according to atomic force microscopy and SEM characterization (Supporting Information Fig. S3). The chemically prepared GO was readily dispersible in water, mainly because of the presence of hydrophilic groups such as hydroxyl (3420 cm^{-1}) and carboxylic groups (1740 and 1250 cm^{-1}) at the GO surface; these were confirmed by FT-IR [Supporting Information Fig. S3(c)].

The working principle of our strategy is represented in Scheme 2. pArg is introduced on the surface of CPN via electrostatic interaction to obtain pArg@CPN. The nanohybrids were fabricated by assembling pArg@CPN on GO nanosheets via electrostatic interaction. The pArg on the surface of the CPN serves as a linker to improve the immobilization of CPN

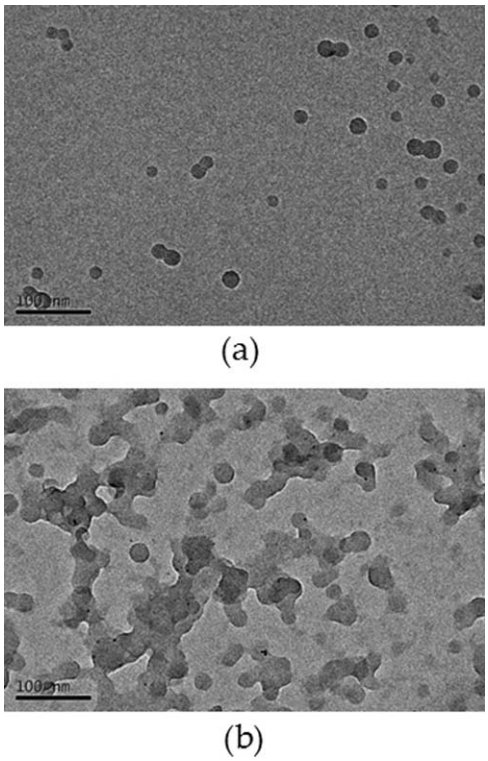

FIGURE 2 TEM images of (a) CPN from CP2 and (b) pArg@CPN (scale bar 100 nm).

on GO. Simultaneously, the original green emission of pArg@CPN is almost quenched because of energy transfer to the electron-accepting GO. Upon exposure to trypsin, CPN can be released from the hybrid because the surrounding pArg is selectively hydrolyzed by the enzymatic action of trypsin, resulting in a weakening of the electrostatic interaction between GO and pArg@CPN. Finally, the nonemissive nanohybrid disrupts and the released pArg@CPN becomes re-emissive because of its trypsin activity.

Once the positive pArg@CPN is immobilized to the surface of the negative GO, the nanohybrid can be easily formed via electrostatic interaction. As a result, the fluorescence of the resultant GO-pArg@CPN nanohybrid is quenched because of charge–transfer interactions between the pArg@CPN and GO.[10(a),16] Figure 3 shows the emission spectral change of GO-pArg@CPN according to the concentration of GO. About 80% quenching is observed in the presence of GO, caused by photo-induced electron or energy transfer. Further complete quenching is possible using GO. In such a case, the facile recovery of fluorescence in the presence of trypsin will be problematic because of the large amount of GO.

After preparation of the nanohybrid of GO-pArg@CPN, trypsin was added to the mixture solution and the changes in fluorescence intensity were observed as the concentration of trypsin was increased. In the concentration range of 0–25 μg/mL in HEPES buffer solutions, the fluorescence intensity of GO-pArg@CPN at 496 nm increased to 80% of the original intensity of pArg@CPN [Fig. 4(a)]. The plot of the trypsin concentration is linearly proportional to the intensity change with a correlation coefficient (R) of 0.996 [Fig. 4(b)]. The limit of detection (3σ/slope) was found to be 0.827 μg/mL, as estimated according to a method reported previously.[17] The spectral response was clearly attributed to the enzymatic activity

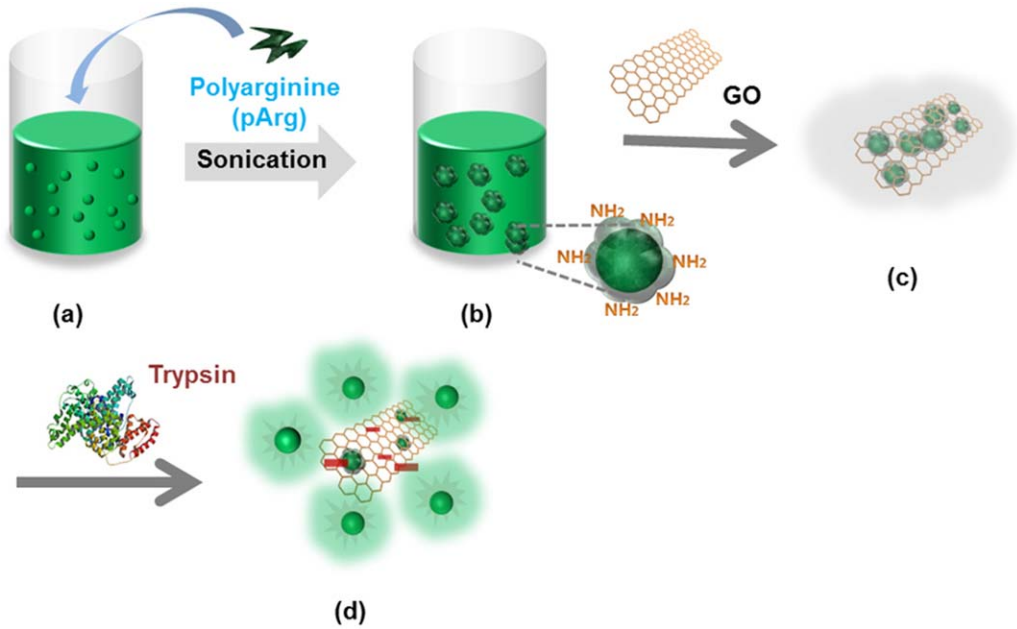

SCHEME 2 Schematic illustration for the detection of trypsin using nanohybrid of pArg@CPN and GO: (a) Green-emitting CPN; (b) pArg@CPN; (c) fluorescence-quenched pArg@CPN via interaction between GO and pArg@CPN; (d) revival of green fluorescence of pArg@CPN via hydrolysis of linker pArg by enzymatic action of trypsin, leading to releasing pArg@CPN. [Color figure can be viewed in the online issue, which is available at wileyonlinelibrary.com.]

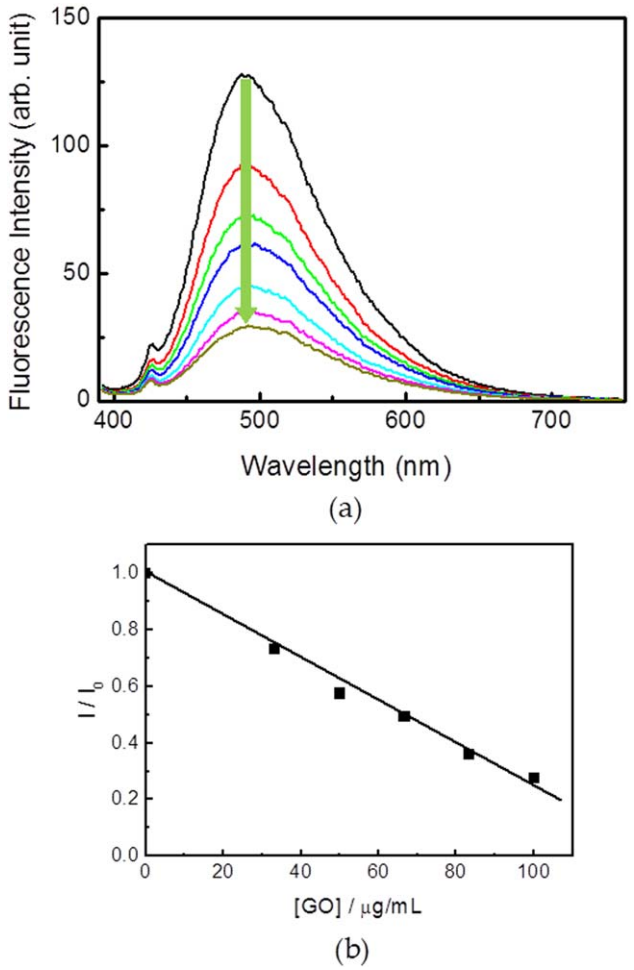

FIGURE 3 (a) Changes in emission intensity and (b) linear relationship of pArg@CPN in the presence of GO with various concentrations in 20 mM HEPES buffer at pH = 7.4 (top to bottom [GO] = 0; 33.3; 50.1; 66.7; 83.4; 100.1; 116.8 μg/mL). Excitation wavelength λ_{ex} = 380 nm. I_o and I correspond to emission intensity at 491 nm in the absence and presence of GO, respectively. [Color figure can be viewed in the online issue, which is available at wileyonlinelibrary.com.]

of trypsin. In this mechanism, the trypsin cleaves a peptide chain at the carboxyl side of the pArg@CPN and, thus, weakens the electrostatic interaction between the pArg@CPN and GO, resulting in the release of CPN from GO.

To evaluate the effect of trypsin activity further, the increase in fluorescence was investigated according to incubation time. About 40 min of incubation time is sufficient for trypsin activity for this emission-enhancement system [Supporting Information Fig. S4(a)]. To investigate whether this detection method can enhance the selectivity, control experiments were carried out using lysozyme, glucose oxidase (GOx), bovine serum albumin (BSA), and pepsin instead of trypsin in HEPES buffer solutions, as shown in Supporting Information Figure S4. Other proteins and proteases did not show obvious fluorescence enhancement, because other proteins cannot hydrolyze the pArg and, thus, cannot release the CPN from the GO-pArg@CPN. The relative selectivity of this system toward trypsin detection is illustrated in Figure 5, which shows that more than twofold emission enhancement can be attained compared with other proteins. To the best of our knowledge, the nanohybrid of GO and pArg-encapsulated CPN using the specific activity of trypsin has not been exploited previously for the turn-on detection of trypsin.

CONCLUSIONS

This work demonstrates a new assay based on the control of interaction between GO and pArg-encapsulated CPN for trypsin detection, in which CPN were prepared from a newly synthesized conjugated polymer. By means of nanohybrid formation of GO and pArg@CPN, the fluorescence of the

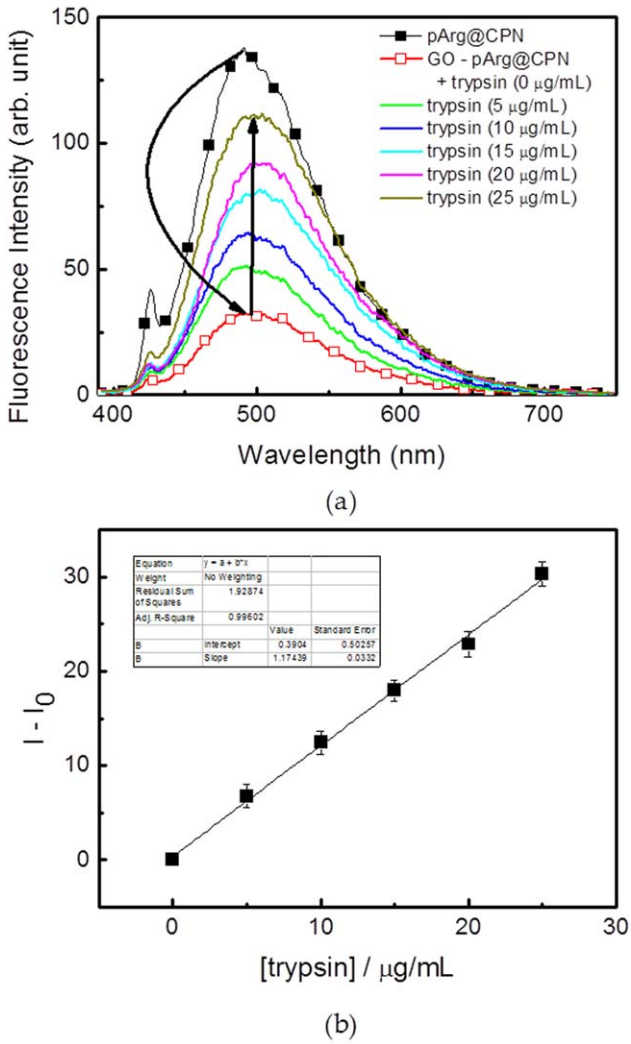

FIGURE 4 (a) Changes in emission intensity and (b) linear relationship of GO-pArg@CPN in the presence of trypsin with various concentrations in 20 mM HEPES buffer at pH = 7.4. [GO] = 100.1 μg/mL; [trypsin] = 0; 5; 10; 15; 20; 25 μg/mL (from bottom to top). Excitation wavelength λ_{ex} = 380 nm. I_o and I correspond to emission intensity at 491 nm in the absence and presence of GO, respectively. [Color figure can be viewed in the online issue, which is available at wileyonlinelibrary.com.]

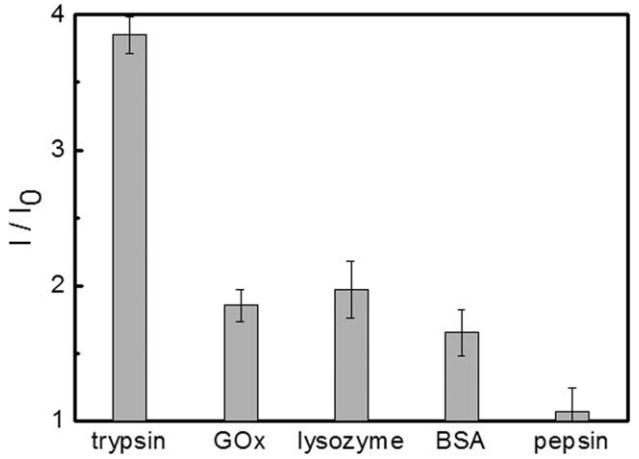

FIGURE 5 Selectivity for trypsin compared to other proteins and enzymes in 20 mM HEPES buffer at pH = 7.4. [GO] = 100.1 μg/mL; [proteins] = 60.0 μg/mL. Excitation wavelength λ_{ex} = 380 nm I_o and I correspond to emission intensity at 491 nm in the absence and presence of GO, respectively.

pArg@CPN was effectively suppressed by GO. The presence of trypsin selectively degraded pArg and, in turn, destroyed the fluorescence-quenched nanohybrid assay, resulting in the release of CPN. Therefore, fluorescence could be recovered according to the concentration of trypsin. Because pArg was employed as the linker of CPN and GO as well as selective degrading sites by trypsin, unique selectivity was observed over other proteins, which indicates this system can be an efficient tool for potein sensing.

ACKNOWLEDGMENTS

Financial support from National Research Foundation of Korea (NRF) funded by Korean government via Basic Science Research Program (2012R1A2A2A01004979) is gratefully acknowledged.

REFERENCES AND NOTES

1 (a) J. Zhang, Y. Tang, K. Lee, M. Ouyang, *Science* **2010**, *327*, 1634–1638; (b) S.-H. Hu, X. Gao, *J. Am. Chem. Soc.* **2010**, *132*, 7234–7237; (c) M. R. Jones, K. D. Osberg, R. J. Macfarlane, M. R. Langille, C. A. Mirkin, *Chem. Rev.* **2011**, *111*, 3736–3827; (d) C. D. M. Donega´, *Chem. Soc. Rev.* **2011**, *40*, 1512–1546; (e) Y. Jin, X. Gao, *Nat. Nanotechnol.* **2009**, *4*, 571–576; (f) M. R. Buck, J. F. Bondi, R. E. Schaak, *Nat. Chem.* **2012**, *4*, 37–44.

2 (a) K. Pu, K. Li, J. Shi, B. Liu, *Chem. Mater.* **2009**, *21*, 3816–3822; (b) L. P. Fernando, P. K. Kandel, J. Yu, J. McNeill, P. C. Ackroyd, K. A. Christensen, *Biomacromolecules* **2010**, *11*, 2675–2682; (c) T. Vokatá, J. H. Moon, *Macromolecules* **2013**, *46*, 1253–1259; (d) C. Wu, T. Schneider, M. Zeigler, J. Yu, P. G. Schiro, D. R. Burnham, J. D. McNeill, D. T. Chiu, *J. Am. Chem. Soc.* **2010**, *132*, 15410–15417; (e) C. Wu, B. Bull, C. Szymanski, K. Christensen, J. McNeill, *ACS Nano* **2008**, *2*, 2415–2423; (f) A. Kaeser, A. P. H. Schenning, *Adv. Mater.* **2010**, *22*, 2985–2997; (g) J. Pecher, S. Mecking, *Chem. Rev.* **2010**, *110*, 6260–6279; (h) P. Howes, M. Green, J. Levitt, K. Suhling, M. Hughes, *J. Am. Chem. Soc.* **2010**, *132*, 3989–3996.

3 (a) Y. Jin, F. Ye, C. Wu, Y.-H. Chan, D. T. Chiu, *Chem. Commun.* **2012**, *48*, 3161–3163; (b) Y.-H. Chan, F. Ye, M. E. Gallina, X. Zhang, Y. Jin, I.-C. Wu, D. T. Chiu, *J. Am. Chem. Soc.* **2012**, *134*, 7309–7312; (c) J. Geng, J. Liu, J. Liang, H. Shi, B. Liu, *Nanoscale* **2013**, *5*, 8593–8601; (d) C. Wu, Y. Jin, T. Schneider, D. R. Burnham, P. B. Smith, D. T. Chiu, *Angew. Chem. Int. Ed.* **2010**, *49*, 9436–9440.

4 (a) D. Li, R. B. Kaner, *Science* **2008**, *320*, 1170–1171; (b) D. A. Dikin, S. Stankovich, E. J. Zimney, R. D. Piner, G. H. B. Dommett, G. Evmenenko, S. T. Nguyen and R. S. Ruoff, *Nature* **2007**, *448*, 457–460; (c) K. S. Novoselov, A. K. Geim, S. V. Morozov, D. Jiang, Y. Zhang, S. V. Dubonos, I. V. Grigorieva, A. A. Firsov, *Science* **2004**, *306*, 666–669; (d) M. J. Allen, V. C. Tung, R. B. Kaner, *Chem. Rev.* **2010**, *110*, 132–145.

5 (a) E. Morales-Naváez, A. Merkoçi, *Adv. Mater.* **2012**, *24*, 3298–3308; (b) S. Guo, S. Dong, *J. Mater. Chem.* **2011**, *21*, 18503–18516; (c) Y. Xu, A. Malkovskiy, Y. Pang, *Chem. Commun.* **2011**, *47*, 6662–6664; (d) Y. Lin, Y. Tao, F. Pu, J. Ren, Z. Qu, *Adv. Funct. Mater.* **2011**, *21*, 4565–4572; (e) J. Geng, L. Zhou, B. Liu, *Chem. Commun.* **2013**, *49*, 4818–4820; (f) X. Qi, H. Li, J. W. Y. Lam, X. Yuan, J. Wei, B. Z. Tang, H. Zhang, *Adv. Mater.* **2012**, *24*, 4191–4195.

6 (a) K. Yamashita, K. Mimori, H. Inoue, *Cancer Res.* **2003**, *63*, 6575–6578; (b) M. Hirota, M. Ohmuraya, H. J. Baba, *Gastroenterology* **2006**, *41*, 832–836.

7 (a) H. Yamamoto, S. Iku, Y. Adachi, A. Imsumran, H. Taniguchi, K. Nosho, Y. Min, S. Horiuchi, M. Yoshida, F. Itoh, K. Imai, *J. Pathol.* **2003**, *199*, 176–184; (b) G. H. Caughey, *Immunol. Rev.* **2007**, *217*, 141–154.

8 (a) J. V. Olsen, S. E. Ong, M. Mann, *Mol. Cell. Proteomics* **2004**, *3*, 608–614; (b) Q. Zhu, R. Zhan, B. Liu, *Macromol. Rapid Commun.* **2010**, *31*, 1060–1064; (c) J. H. Wosnick, C. M. Mello, T. M. Swager, *J. Am. Chem. Soc.* **2005**, *127*, 3400–3405.

9 (a) M. Li, X. Zhou, S. Guo, N. Q. Wu, *Biosens. Bioelectron.* **2013**, *43*, 69–74; (b) M. Li, Q. Wang, X. Shi, L. A. Hornak, N. Q. Wu, *Anal. Chem.* **2011**, *83*, 7061–7065.

10 (a) J. Balapanuru, J.-X. Yang, S. Xiao, Q. Bao, M. Jahan, L. Polavarapu, J. Wei, Q.-H. Xu, K. P. Loh, *Angew. Chem. Int. Ed.* **2010**, *49*, 6549–6553; (b) X. Xu, J. Huang, J. Li, J. Yan, J. Qin, Z. Li, *Chem. Commun.* **2011**, *47*, 12385–12387; (c) H.-L. Zhang, X.-L. Wei, Y. Zang, J.-Y. Cao, S. Liu, X.-P. He, Q. Chen, Y.-T. Long, J. Li, G.-R. Chen, K. Chen, *Adv. Mater.* **2013**, *25*, 4097–4101; (d) E. Ahmed, S. W. Morton, P. T. Hammond, T. M. Swager, *Adv. Mater.* **2013**, 25, 4504–4510; (e) X. Wang, F. He, L. Li, H. Wang, R. Yan, L. Li, *ACS Appl. Mater. Interfaces* **2013**, *5*, 5700–5708.

11 Z.-G. Zhang, K.-L. Zhang, G. Liu, C.-X. Zhu, K.-G. Neoh, E.-T. Kang, *Macromolecules* **2009**, *42*, 3104–3111.

12 W. S. Hummers, R. E. Offeman, *J. Am. Chem. Soc.* **1958**, *80*, 1339–1339.

13 C. Wu, S. J. Hansen, Q. Hou, J. Yu, M. Zeigler, Y. Jin, D. R. Burnham, J. D. McNeill, J. M. Olson, D. T. Chiu, *Angew. Chem. Int. Ed.* **2011**, *50*, 3430–3434.

14 H. Shi, H. Sun, H. Yang, S. Liu, G. Jenkins, W. Feng, F. Li, Q. Zhao, B. Liu, W. Huang, *Adv. Funct. Mater.* **2013**, *23*, 3268–3276.

15 R. J. Hunters, Zeta Potential in Colloid Science: Principles and Applications, Academic Press: London, **1981**.

16 (a) Y. X. Xu, H. Bai, G. W. Lu, C. Li, G. Q. Shi, *J. Am. Chem. Soc.* **2008**, *130*, 5856–5857; (b) Y. Y. Liang, D. Q. Wu, X. L. Feng, K. Müllen, *Adv. Mater.* **2009**, *21*, 1679–1683.

17 V. Thomsen, D. Schatzlein, D. Mercuro, *Spectroscopy* **2003**, *18*, 112–114.